Available online at www.sciencedirect.com

SCIENCE DIRECT

European Journal of Pharmacology 516 (2005) 187 – 196

www.elsevier.com/locate/ejphar

Mitochondrial dysfunction is related to necrosis-like programmed cell death induced by A23187 in CEM cells

Keigo Hamahata[a], Souichi Adachi[a,*], Hiroshi Matsubara[a], Masayuki Okada[a], Tsuyoshi Imai[a], Ken-ichiro Watanabe[a], Shin-ya Toyokuni[b], Masaki Ueno[c], Shigeo Wakabayashi[d], Yuki Katanosaka[d], Satoshi Akiba[e], Masaru Kubota[f], Tatsutoshi Nakahata[a]

[a]*Department of Pediatrics, Graduate School of Medicine, Kyoto University, 54 Kawahara-cho, Shogoin, Sakyo-ku, Kyoto 606-8507, Japan*
[b]*Department of Pathology, Graduate School of Medicine, Kyoto University, Japan*
[c]*Department of Pathology and Host defense, Kagawa Medical University, Japan*
[d]*Department of Molecular Physiology, National Cardiovascular Center Research Institute, Japan*
[e]*Department of Pathological Biochemistry, Kyoto Pharmaceutical University, Japan*
[f]*Department of Pediatrics, Kobe City General Hospital, Japan*

Received 5 April 2005; accepted 11 April 2005

Abstract

We have previously reported that calcium ionophore A23187 differentially induces necrosis in CEM cells, a T-lymphoblastic leukemia cell line, and apoptosis in HL60 cells, a promyelocytic leukemia cell line. Stimulation with VP16, however, induces typical apoptosis in both cell lines. Necrosis in CEM cells, characterized by cell shrinkage and clustering, began within 5 min of treatment. Swelling of the mitochondria, lumpy chromatin condensation and intact plasma membranes were evident by electron microscopy. These A23187-mediated changes in CEM cells were suppressed by clonazepam or CGP37157, inhibitors of the mitochondrial Na^+/Ca^{2+} exchanger. The changes, however, were not affected by cyclosporin A, an inhibitor of the mitochondrial permeability transition pore. In both CEM and HL60 cells, intra-cellular calcium increased with similar amplitude within 1 min of treatment with 2 μM A23187. Intra-mitochondrial calcium increased with clonazepam pre-treatment alone in both CEM and HL60 cells. However, intra-mitochondrial calcium did not change drastically in response to A23187 in CEM or HL60 cells, either untreated or pre-treated with clonazepam. A23187 induces necrosis in CEM cells concurrent with mitochondrial dysfunction, which is independent of the mitochondrial permeability transition, but affected by intra-mitochondrial calcium, while HL60 cells lack these early changes. Differences in the responses to A23187 between these two cell lines might derive from differences in the susceptibility of the mitochondrial membrane to rapid increases in intra-cellular calcium.

Keywords: Apoptosis; Necrosis; Mitochondria; Calcium ionophore; Clonazepam; Bcl-2

1. Introduction

Cells lose viability in response to various stimuli; such cell death can occur within minutes or take hours to develop, depending on both the cell type and stimulus. Apoptosis involves the execution of a pre-programmed sequence of cellular events (Fiers et al., 1999) over the course of several hours, leading to the orderly resorption of unneeded cells. In contrast to apoptosis, necrosis is thought to be accidental and unregulated, occurring with a rapid onset as a consequence of ATP depletion, the acute disruption of cellular metabolism, or ion dysregulation. These signals lead to mitochondrial and cellular swelling, followed by plasma membrane destruction (Fiers et al., 1999). The molecular mechanisms of apoptosis have been well studied (Kroemer and Reed, 2000), while less is known about the processes involved in necrosis. Recent reports, however, have detailed a caspase-independent mode of cell

* Corresponding author. Tel.: +81 75 7513301; fax: +81 75 7522361.
E-mail address: sadachi@kuhp.kyoto-u.ac.jp (S. Adachi).

0014-2999/$ - see front matter © 2005 Elsevier B.V. All rights reserved.
doi:10.1016/j.ejphar.2005.04.018

death with necrotic morphology, which appears to be regulated by cellular intrinsic programs (Blagosklonny, 2000; Chi et al., 1999; Jambrina et al., 2003; Kitanaka and Kuchino, 1999; Leist and Jaattela, 2001; Velde et al., 2000).

Calcium is understood to play an important role in various types of cell injury (Berridge et al., 1998; Ichas and Mazat, 1998; Lemasters et al., 1998). Calcium ionophore A23187, which induces diverse responses in many cell types (Matsubara et al., 1994; Qian et al., 1999; Zhu and Loh, 1995), has often been used in models of calcium-dependent cytotoxicity. A23187 induces necrosis in CEM cells, a T-lymphoblastic leukemia cell line, but apoptosis in HL60 cells, a promyelocytic leukemia cell line (Matsubara et al., 1994). In contrast, VP16, a topoisomerase II inhibitor, induces typical apoptosis in both cell lines, which means there is no intrinsic defect in the apoptotic mechanisms in CEM cells. We examined the differences in the responses of these two cell lines to A23187 through examination of their morphology, caspase activation, mitochondrial membrane potential, and plasma membrane permeability.

We found that the morphological changes induced in CEM cells by A23187, including cell shrinkage and clustering, appeared within 5 min of treatment. These features, however, were subsequently followed by the appearance of typical necrotic morphology. HL60 cells lacked the early changes in morphology, instead requiring at least 3 h of continuous exposure to A23187 for apoptotic initiation. To examine the molecular mechanisms controlling this necrosis-like cell death, we explored changes in the intra-cellular and intra-mitochondrial calcium concentration in CEM and HL60 cells following treatment with A23187.

2. Materials and methods

2.1. Cell lines and transfection

CEM, a T-lymphoblastic line, and HL60, a promyelocytic leukemia line, were obtained from JCRB (Osaka, Japan). Cells were cultured in RPMI1640 (Gibco-BRL, Grand Island, NY) supplemented with 10% fetal bovine serum (Gibco-BRL). Human *Bcl-2* cDNA was a kind gift from Y. Tsujimoto (Osaka University, Japan) and was transfected into CEM cells by electroporation. Expression of Bcl-2 protein was confirmed by Western blot analysis.

2.2. Reagents

A23187, cyclosporin A, and propidium iodide were purchased from Sigma-Aldrich Chemical Co. (St. Louis, MO). CGP37157 was acquired from Biomol Research Laboratories Inc. (PA, USA). $DiOC_6(3)$, fluo-3 AM, and rhod-2 AM were obtained from Molecular Probes (OR, USA). DEVD-AMC was procured from Peptide Institute (Osaka, Japan). Clonazepam was kindly provided by SUMITOMO Pharmacol. Co. (Osaka, Japan). [^{3}H] Arachidonic acid (209 Ci/mmol) was purchased from Amersham Pharmacia Biotech (Buckinghamshire, UK).

2.3. Cell morphology

Cytospin preparation was performed at $80\times g$ for 1 min using Cytospin 2 (Shandon, UK). Cellular morphology was examined under an optical microscope after May-Giemsa staining. For electron microscopic observation (Toyokuni et al., 1989), 5×10^6 cells were isolated. Cell samples were fixed with 2% glutaraldehyde in 0.05 M phosphate buffer. Samples were washed in isotonic phosphate-buffered sucrose solution, refixed in a phosphate-buffered solution of 1% osmium tetroxide, dehydrated in a graded ethanol series, and embedded in Epon 812. Samples were sectioned with a glass knife on a Sorvall MT-5000 ultramicrotome, and then mounted on copper grids coated with polyvinylformal. Samples were stained with uranyl acetate and lead citrate, and then observed using a Hitachi HU-12A electron microscope.

2.4. Caspase-3-like protease activity assay

Caspase-3-like protease activity was measured using a Fluorometer 1420 ARVO SX FL (Wallac, Turku, Finland) with DEVD-AMC, a specific substrate of caspase-3 (Yamashita et al., 1999).

2.5. FACS analysis with $DiOC_6(3)$/propidium iodide

Flow cytometric analysis was performed on a FACS Calibur flow cytometer (Becton Dickinsons, Bedford, MA) following staining of samples with propidium iodide, an indicator of plasma membrane permeability, and $DiOC_6(3)$, an indicator of mitochondrial membrane potential. Five hundred thousand cells were mixed with propidium iodide (5 μg/ml) and $DiOC_6(3)$ (20 nM), and then analyzed after a 10-min incubation in 37 °C.

2.6. Calcium assay

To measure intra-cellular calcium, we utilized a calcium-sensitive fluorescent dye, fluo-3, suitable for measuring rapid dynamic changes in intra-cellular calcium, using a flow cytometer (Fanelli et al., 1999). Cells were loaded with fluo-3 by incubating 1×10^7 cells with 3 μM fluo-3 AM for 30 min at 37 °C. Following extensive washing, samples were analyzed using a FACS Calibur. While quantitative measurement of intra-mitochondrial calcium using rhod-2 with confocal microscopy has been applied for fixed adherent cells (Muriel et al., 2000), it is difficult to apply this technique to CEM and HL60 suspension cells. Therefore, we have developed a method for analyzing rhod-2-loaded cells using a FACS Calibur. Rhod-2 AM was first reduced with $NaBH_4$, and then loaded into 1×10^7 cells at 5 μM for 1 h at 37 °C. Following extensive washing, the cells were incubated for 6 h in 37 °C to allow sequestration of rhod-2 into mitochondria. Samples were analyzed by flow cytometry.

While it is impossible to quantify the absolute values of calcium concentrations, as neither fluo-3 nor rhod-2 are ratiometric dyes such as fura-2 or indo-1, fluorescence changes reflect the dynamic changes in both intra-cellular and intra-mitochondrial calcium. Relative values of fluo-3 or rhod-2 fluorescence are indicated as the ratio of sampled values to the

initial fluorescence values, to indicate the calcium dynamics in response to each agent.

2.7. Arachidonic acid release

CEM cells (6×10^6 cells/ml) were incubated with [^{3}H] arachidonic acid (1 μCi/ml) at 37 °C for 2 h. After being washed, the labeled cells were stimulated with 2 μM A23187 for 10 or 30 min in a final volume of 200 μl. The reaction was terminated by adding 2 ml of chloroform/methanol/HCl (200:200:1, v/v/v). Lipids were extracted and separated by thin-layer chromatography on a silica gel G plate with petroleum ether/diethyl ether/acetic acid (40:40:1, v/v/v) as the development system. The area corresponding to free fatty acid or other lipids was scraped off, and the radioactivity was measured by liquid scintillation counting. The radioactivity of fatty acid was corrected by adjusting the total radioactivity to 2.0×10^5 dpm (Akiba et al., 2004).

2.8. Immunoblot analysis of NCX isoforms

CEM and HL60 cells and tissues from mouse brain and ventricular muscles were homogenized by physcotron (NITI-ON, Japan) in RIPA lysis buffer containing 20 mM HEPES (pH 7.4), 150 mM NaCl, 1% sodium deoxycholate, 1% Triton X-100, 0.1% SDS, 2 μg/ml leupeptin, 1 μg/ml aprotinin, 200 μM phenylmethylsulphonyl fluoride, and 200 μM benzamidine hydrochloride. The lysates were centrifuged at 100,000×g for 20 min. The supernatants were subjected to SDS-PAGE on an 8.5% gel and then transferred to Immobilon membranes (Millipore). After blocking, incubation with polyclonal antibodies against NCX isoforms (Iwamoto et al., 1996) and washing, protein signals were visualized using an enhanced chemiluminescence detection system (Nakarai tesque).

3. Results

3.1. Morphology

Morphological changes of CEM and HL60 cells in response to A23187 were observed (Fig. 1A). The morphology of CEM cells treated for 6 h with 2 μM A23187 showed characteristics typical of necrosis, including cell swelling and rupture. Within 10 min, CEM cells treated with 2 μM A23187 exhibited the peculiar morphology of cell shrinkage and clustering, which we considered to be early stage of necrosis. HL60 cells treated for 6 h with 2 μM A23187, however, showed characteristics typical of apoptosis, including cell shrinkage, chromatin condensation and nuclear fragmentation. In the first 10 min, HL60 cells treated with 2 μM A23187 did not show any remarkable morphological changes. CEM cells treated for 6 h with 10 μg/ml VP16 exhibited the cellular changes typical of apoptosis, indicating that CEM cells retained the capacity to undergo apoptosis (data not shown).

The dose–response relationship of CEM cells (Fig. 1B) and HL60 cells (Fig. 1C) in response to various concentration of A23187 was examined. CEM cells were treated for 6 h either with 0 μM, 0.5 μM, 1 μM, 2 μM or 4 μM of A23187 and examined morphologically. CEM cells treated with increasing concentration of A23187 exhibited increasing number of cells with necrotic morphology, but almost none with apoptotic morphology. In contrast, HL60 cells treated with increasing concentration of A23187 exhibited increasing number of cells with apoptotic morphology, but almost none with necrotic morphology. With much higher concentration of A23187 at 20 μM, HL60 cells also exhibited cells with necrotic morphology (data not shown).

The cellular and mitochondrial ultrastructural features of this early necrosis in CEM cells were observed by electron microscopy (Fig. 1D). The nuclei and mitochondria of untreated CEM cells appeared normal. CEM cells treated with 2 μM A23187 for 6 h showed the phenotypic changes associated with necrosis: destruction of the plasma membrane, condensation of nuclear chromatin and enlarged electron-dense mitochondria. CEM cells treated with 2 μM A23187 for 10 min retained an intact plasma membrane, but demonstrated lumpy chromatin condensation and enlarged electron-dense mitochondria, characteristic of necrosis (Leist and Jaattela, 2001). CEM cells treated for 6 h with 10 μg/ml VP16 showed typical apoptotic morphology, including an intact plasma membrane, condensed chromatin and mitochondrial destruction. Under the same conditions of treatment with 2 μM A23187 for 6 h, HL60 cells exhibited morphology typical of apoptosis, similar to the characteristics of CEM cells treated with 10 μg/ml VP16 (data not shown).

3.2. Caspase-3-like protease activation

Caspase-3-like protease activities were measured (Fig. 2). Caspase-3 activation was demonstrated in both HL60 cells and CEM cells treated for 6 h with 10 μg/ml VP16. Caspase-3 activation was demonstrated in HL60 cells, but not in CEM cells, treated for 6 h with 2 μM A23187. Caspase-3 activation was absent in both HL60 cells and CEM cells treated for 10 min with 2 μM A23187.

3.3. Flow cytometric analysis

Mitochondrial membrane potential was next analyzed by flow cytometry (Fig. 3). Cells were stained with propidium iodide (PI), an indicator of plasma membrane permeability, and $DiOC_6(3)$, an indicator of mitochondrial membrane potential. Prior to treatment, intact CEM cells exhibited a $DiOC_6(3)^{high}/PI^-$ pattern. CEM cells treated with 2 μM A23187 for 6 h exhibited a $DiOC_6(3)^{low}/PI^+$ pattern. This staining pattern may correspond to a necrotic population in agreement with the morphological analysis of the same sample. CEM cells treated with 2 μM A23187 for 10 min contained a population of $DiOC_6(3)^{low}/PI^-$ and a population of $DiOC_6(3)^{low}/PI^+$. CEM cells treated with 10 μg/ml VP16 for 6 h exhibited a $DiOC_6(3)^{low}/PI^-$ pattern, which likely corresponded to an apoptotic population as deduced from the morphological analysis of these cells.

3.4. Wash out experiment

To investigate the kinetics of the onset of necrosis and apoptosis, cells were exposed to 2 μM A23187 for 10 min, and then immediately washed with medium. Morphological and flow cytometric findings were compared with those of cells under continuous exposure to 2 μM A23187 for 6 h (Fig. 4). CEM cells exposed to 2 μM A23187 for only 10 min contained a significant population of necrotic cells ($DiOC_6(3)^{low}/PI^+$) after an additional 6 h of incubation (Fig. 4A). HL60 cells exposed to 2 μM A23187

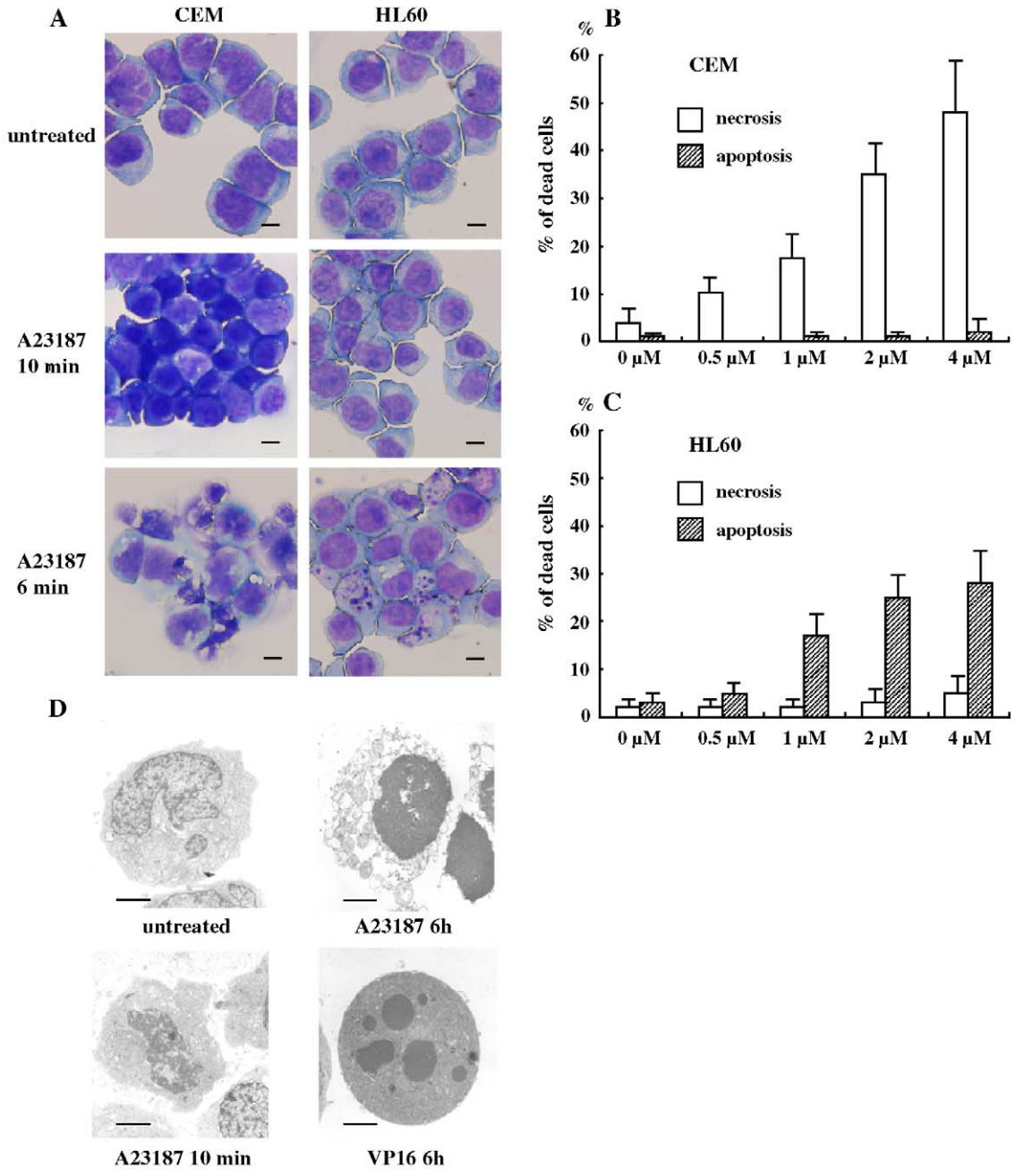

Fig. 1. Morphology of the response of CEM and HL60 cells to A23187. (A) Cytospin morphology of CEM cells (left) and HL60 cells (right) observed under an optical microscope. Untreated cells, cells treated with 2 μM A23187 for 10 min and cells treated with 2 μM A23187 for 6 h are shown from top to bottom, respectively. The scale bars represent 10 μm. (B, C) The dose–response relationship of CEM cells (B) and HL60 cells (C) in response to various concentration of A23187. The percentage of the cells with necrotic morphology (open bars) and the cells with apoptotic morphology (closed bars) are shown. Data are means ± S.D. from four independent experiments. (D) Ultrastructure of CEM cells observed by electron microscopy. Untreated cells, cells treated with 2 μM A23187 for 10 min, cells treated with 2 μM A23187 for 6 h and cells treated with 10 μg/ml VP16 for 6 h are shown. The scale bars represent 10 μm.

for 6 h exhibited a significant population of apoptotic (DiO-$C_6(3)^{low}/PI^-$) cells; however, those exposed to A23187 for 10 min did not exhibit a significant population of either apoptotic or necrotic cells (Fig. 4B). An additional study varying the exposure time revealed that necrosis was rapidly induced within 5 min in CEM cells by 2 μM A23187 treatment (Fig. 5, thick solid line); HL60 cells, however, required at least 3 h of continuous exposure to 2 μM A23187 for the initiation of apoptosis (data not shown).

3.5. The effects of clonazepam, CGP37157 and cyclosporin A on early necrotic change of CEM cells and Bcl-2 overexpressing CEM cells

In order to clarify the role of Bcl-2 in early necrosis, we used Bcl-2-overexpressing CEM cells (CEM/Bcl-2) in comparison with control CEM cells (CEM/Neo). The time-dependence of the changes of the morphology and flow cytometric features of

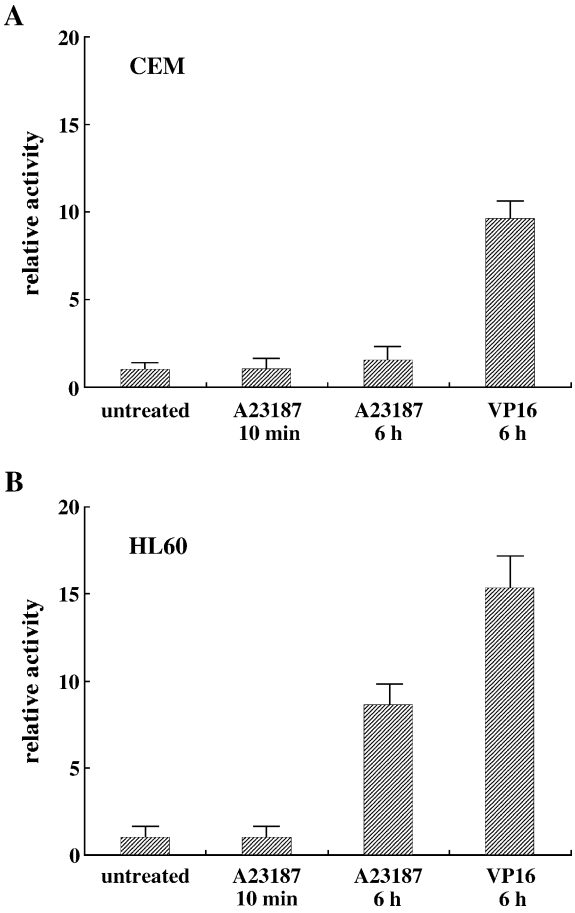

Fig. 2. Caspase-3-like protease activity of CEM cells (A) and HL60 cells (B). Caspase-3-like protease activity of CEM (A) and HL60 (B) cells were analyzed and indicated with the relative value of activity as the ratio to the activity of untreated cells. Relative value of activity of untreated cells, cells treated with 2 μM A23187 for 10 min or 6 h and cells treated with 10 μg/ml VP16 for 6 h are shown from the left to the right, respectively. Data are means ± S.D. from three independent experiments.

CEM/Neo and CEM/Bcl-2 cells exposed to 2 μM A23187 was determined (Fig. 5). CEM cells demonstrated cell shrinkage and clustering morphology within 10 min and typical necrotic morphology after 6 h of exposure to 2 μM A23187 (Fig. 1A). Flow cytometry revealed that a PI^+ population appeared at 10 min, concurrent with the appearance of a PI^- population with decreased $DiOC_6(3)$ staining ($DiOC_6(3)^{low}/PI^-$) (Fig. 3). Time-course analysis of CEM/Neo cells treated with 2 μM A23187, expressed as the percentage of total cells exhibiting a $DiOC_6(3)$-low staining pattern, demonstrated the effective conversion of normal cells to this phenotype within 30 min (Fig. 5A, bold solid line). Time-course analysis of CEM/Bcl-2 cells showed increased necrosis in comparison with control CEM cells in response to A23187 stimulation (Fig. 5B, bold solid line). These morphological and flow cytometric changes induced in CEM/Neo and CEM/Bcl-2 cells by A23187 were almost completely suppressed by pre-incubation with 250 nM clonazepam, an inhibitor of the mitochondrial Na^+/Ca^{2+} exchanger (Griffiths et al., 1997) (Fig. 5A,B, bold dotted line). The subsequent necrosis occurring after 6 h was also inhibited (data not shown). The inhibitory effect of clonazepam was mimicked by CGP37157, another inhibitor of the mitochondrial Na^+/Ca^{2+} exchanger (Scanlon et al., 2000) (Fig. 5A,B, thin solid line). Neither clonazepam nor CGP37157 affected PI and $DiOC_6(3)$ staining pattern by itself (data not shown). Pre-incubation with 1 μM cyclosporin A (Fig. 5A,B, thin dotted line), an inhibitor of the mitochondrial permeability transition pore, did not affect the onset of necrotic change (Nieminen et al., 1996). We also examined the effect of various concentration of cyclosporin A ranging from 100 nM to 10 μM. Neither doses of cyclosporin A affect the onset of necrotic changes induced by A23187 (data not shown).

3.6. Intra-cellular and intra-mitochondrial calcium assay

To determine whether intra-cellular or intra-mitochondrial calcium was responsible for the induction of necrosis, we measured intra-cellular or intra-mitochondrial calcium. A23187 treatment resulted in a rapid rise in intra-cellular calcium within 1 min to a similar degree in both cell lines (Fig. 6A,B, thin solid line). However, intra-cellular calcium was normalized much more rapidly in HL60 cells than in CEM cells. Clonazepam had no effect on intra-cellular calcium by itself (Fig. 6A, B, bold solid line) or on the kinetics of intra-cellular calcium in response to A23187 treatment in either cell line (Fig. 6A,B, bold dotted line). We then measured intra-mitochondrial calcium and found that it increased gradually after exposure to 250 nM clonazepam (Fig. 6C,D, bold solid line), but was not affected by 1 μM cyclosporin A (Fig. 6C,D, bold dotted line) in either cell line. However, intra-mitochondrial calcium was not drastically affected by A23187 in untreated cells (Fig. 6C,D, thin solid line) or cells after pre-incubation with either 250 nM clonazepam (Fig. 6C,D, bold solid

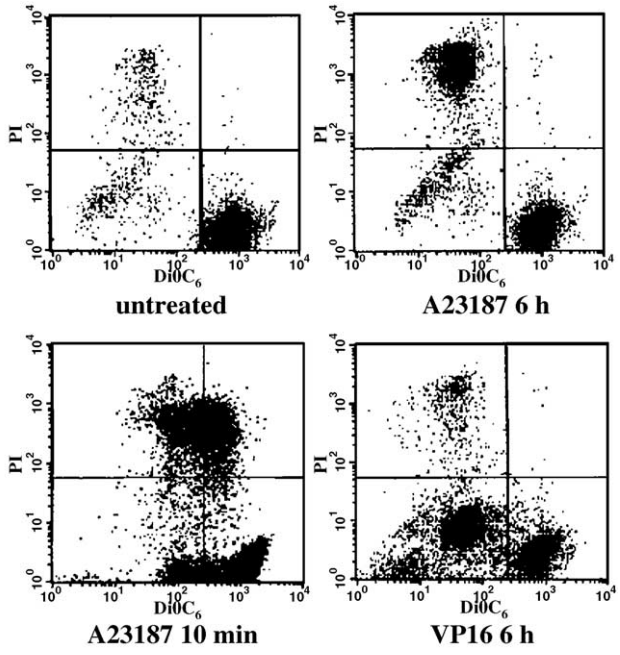

Fig. 3. $DiOC_6(3)$/propidium iodide flow cytometric analysis. CEM cells were stained with propidium iodide and $DiOC_6(3)$, and analyzed by flow cytometry. The vertical axis indicates propidium iodide intensity and the horizontal axis indicates $DiOC_6(3)$ intensity. Analysis of untreated cells, cells treated with 2 μM A23187 for 10 min, cells treated with 2 μM A23187 for 6 h and cells treated with 10 μg/ml VP16 for 6 h are shown.

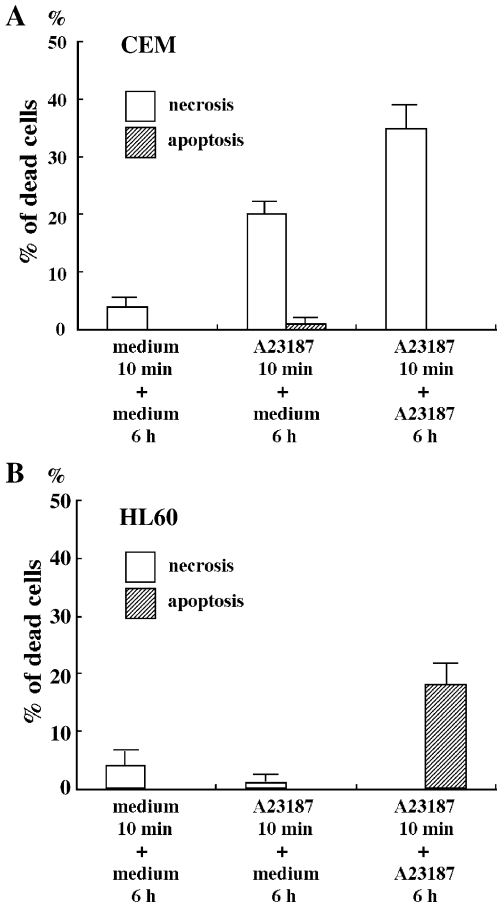

Fig. 4. Wash out experiments. CEM cells (A) and HL60 cells (B) were exposed to 2 μM A23187 for 10 min and immediately washed with fresh medium, and were compared with cells continuously exposed to 2 μM A23187 for 6 h. Open bars indicate the percentage of necrotic population ($DiOC_6(3)^{low}/PI^+$), and closed bars indicate the percentage of apoptotic population ($DiOC_6(3)^{low}/PI^-$). Untreated cells washed and incubated with medium for 6 h (1), cells exposed to 2 μM A23187 for 10 min, washed and incubated with medium for 6 h (2) and cells exposed to 2 μM A23187 for 10 min, washed and incubated again with 2 μM A23187 for 6 h (3) are shown from left to right, respectively. Data are means±S.D. from four independent experiments.

line) or 1 μM cyclosporin A (Fig. 6C,D, bold dotted line) in either cell line. CGP37157 showed similar effects as clonazepam on intra-mitochondrial calcium (data not shown). We also examined intra-cellular and intra-mitochondrial calcium of Bcl-2-overexpressing CEM cells, which showed similar kinetics to control CEM cells in response to A23187 stimulation and similar effect by clonazepam, CGP37157 and cyclosporin A (data not shown).

3.7. Analysis of phospholipase activation

In order to clarify the effect of phospholipase activation in the necrotic process, we examined phospholipase activation in CEM cells treated with A23187. CEM cells labeled with [^{3}H] arachidonic acid were stimulated with 2 μM A23187 for 10 or 30 min. Then, the lipids were extracted, separated by thin-layer chromatography and measured by liquid scintillation counting. Production of diacylglycerol was stimulated but arachidonic acid was not released in CEM cells treated with A23187 (Table 1).

3.8. Immunoblot analysis of NCX isoforms

In order to clarify the effect of Na^+/Ca^{2+} exchanger inhibitors on plasmalemmal NCX isoforms, we examined the expression levels of NCX proteins in CEM and HL60 cells by Western blotting. In CEM and HL60 cells, isoforms of NCX 1, 2, 3 were not detected, which are expressed in the mouse brain or ventricular muscle tissues (Fig. 7).

4. Discussion

Of the two patterns of cell death, considerable data exist detailing the molecular mechanisms of apoptosis, while the mechanisms governing necrosis remain to be elucidated.

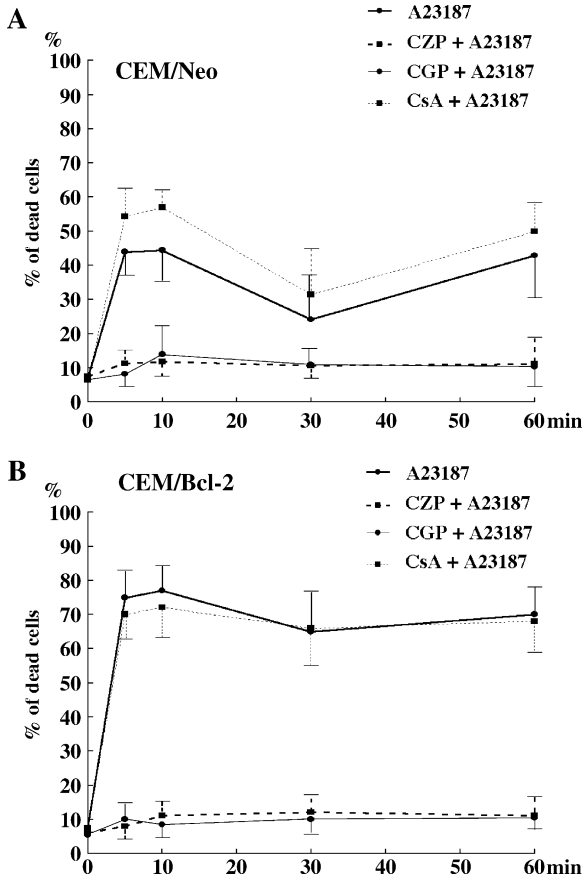

Fig. 5. Time-course analysis of the early necrotic change of CEM cells and Bcl-2-overexpressing CEM cells. The time-dependence of the changes of the flow cytometric features of CEM/Neo cells (A) and CEM/Bcl-2 cells (B) in response to 2 μM A23187 is shown as the percentage of $DiOC_6(3)$-low population. The percentage of the necrotic population of CEM cells without pre-incubation (bold solid line), pre-incubated with 250 nM clonazepam (CZP) (bold dotted line), pre-incubated with 25 nM CGP37157 (CGP) (thin solid line) and pre-incubated with 1 μM cyclosporin A (CsA) (thin dotted line) was measured after the addition of 2 μM A23187. Data are means±S.D. from three independent experiments.

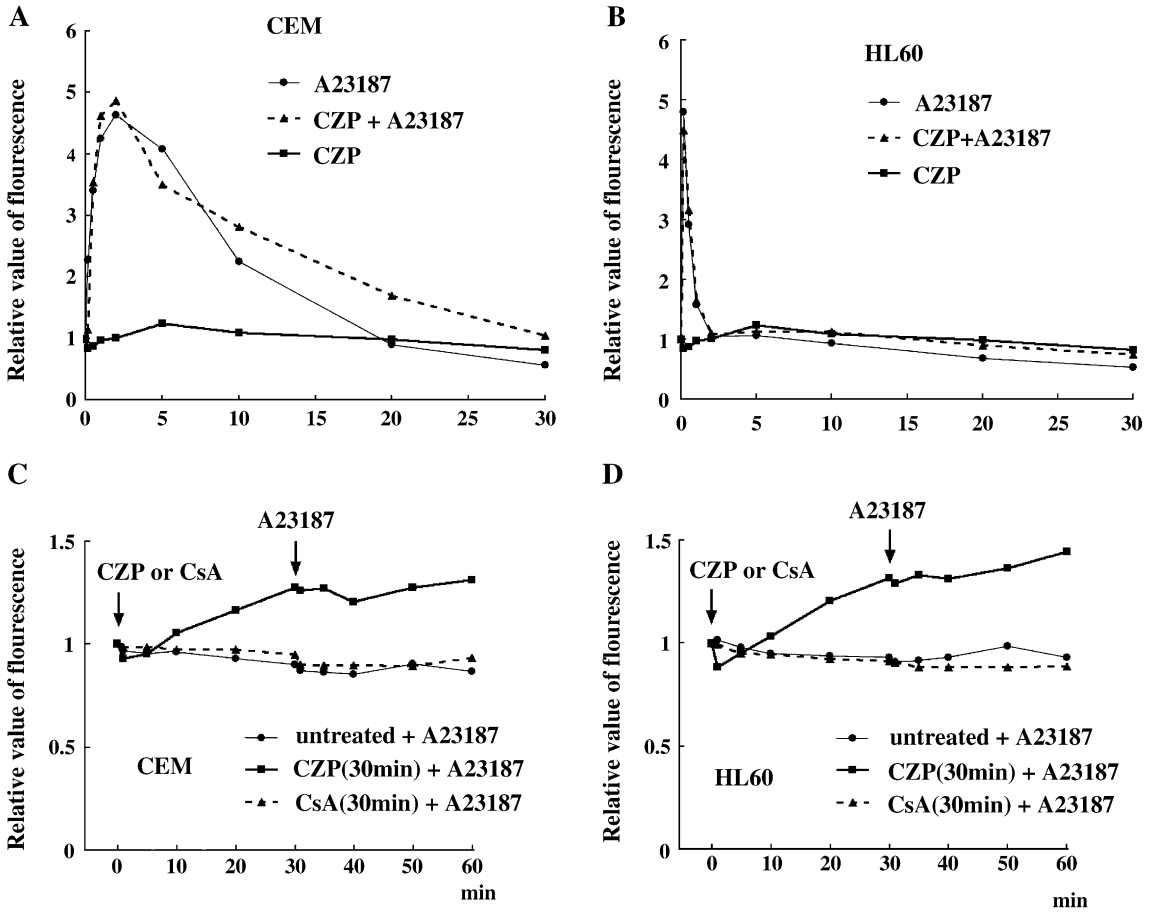

Fig. 6. Intra-cellular and intra-mitochondrial calcium assays. (A, B) For intra-cellular calcium assay, cells were loaded with fluo-3, and analyzed sequentially by flow cytometry after the addition of each agent. The relative value of fluo-3 fluorescence as the ratio to the initial fluorescence is indicated instead of the absolute intra-cellular calcium of CEM cells (A) and HL60 cells (B). Thin solid line, 2 μM A23187-treated cells; bold solid line, 250nM clonazepam (CZP)-treated cells; bold dotted line, 2 μM A23187-treated cells after pre-treatment with 250 nM clonazepam. (C, D) For intra-mitochondrial calcium assay, cells were loaded with rhod-2, and analyzed sequentially by flow cytometry. The relative value of rhod-2 fluorescence as the ratio to the initial fluorescence is indicated instead of the absolute intra-mitochondrial calcium of CEM cells (C) and HL60 cells (D). Thin solid line, cells without pre-treatment and following 2 μM A23187-treatment (arrow head); bold solid line, cells with 250 nM clonazepam pre-treatment and subsequent 2 μM A23187-treatment (arrow head); bold dotted line, cells with 1 μM cyclosporin A (CsA) pre-treatment and subsequent 2 μM A23187-treatment (arrow head). The figures show one of typical results of four independent experiments.

Necrosis is not merely a passive accidental event, but a pre-programmed sequence of events. To clarify the differences in the mechanisms controlling apoptosis and necrosis, we used CEM and HL60 cells, which exhibit different responses to A23187 stimulation (Matsubara et al., 1994). Our experiments indicate that the necrotic process in CEM

Table 1
Arachidonic acid release by A23187 stimulation

	Untreated		2 μM A23187	
	10 min	30 min	10 min	30 min
Diacylglycerol	854	911	1718	1833
Arachidonic acid	2688	2849	2948	2484

The radioactivity of released diacylglycerol and arachidonic acid from CEM cells labeled with [^{3}H] arachidonic acid, which are untreated (left) or treated with 2 μM A23187 (right) for 10 or 30 min are indicated. The radioactivity was corrected by adjusting the total radioactivity to 2.0×10^5 dpm.

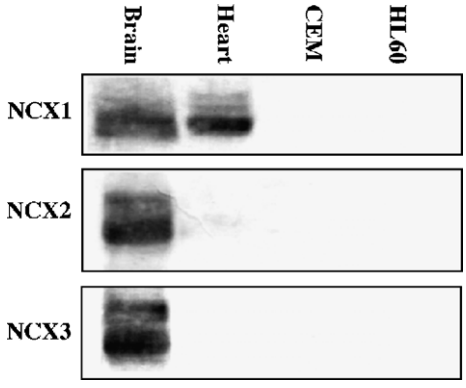

Fig. 7. Protein expression levels of endogenous NCX isoforms. Lysates (5 μg each) prepared from mouse brain, mouse ventricular muscles, CEM and HL60 cells (from the left to the right, respectively) were subjected to immunoblot analysis with antibodies to the Na^+/Ca^{2+} exchanger isoforms, NCX1, NCX2 and NCX3, from top to bottom, respectively.

cells exposed to A23187 is initiated rapidly, while the apoptotic process in HL60 cells under similar conditions is initiated at a later stage. The time courses of the responses of CEM cells to 2 μM A23187 indicate that the necrotic process was initiated within 5 min, and was identifiable by an atypical morphology, that was subsequently replaced by typical necrotic morphology after 6 h. Flow cytometric analysis of PI/$DiOC_6(3)$ staining at this early stage in the necrotic process indicated the transient appearance of a population with a $DiOC_6(3)^{low}/PI^-$ pattern similar to that of apoptotic populations and the subsequent shift to a population with a $DiOC_6(3)^{low}/PI^+$ pattern after 6 h. Mitochondrial dysfunction, demonstrated in the population with decreased $DiOC_6(3)$ intensity, appeared early after stimulation prior to destruction of the plasma membrane. HL60 cells treated with 2 μM A23187 did not exhibit early morphological changes or mitochondrial depolarization.

Electron microscopic observations of this early necrotic stage illustrate some of the morphological characteristics of necrosis (lumpy chromatin condensation and enlarged electron-dense mitochondria in the presence of an intact plasma membrane), reported for caspase-independent cell death (Leist and Jaattela, 2001). These morphological changes in mitochondria and the decrease in mitochondrial membrane potential indicate that A23187 stimulation prompts mitochondria to undergo changes associated with early necrotic state.

This A23187-induced early necrotic change in CEM cells is inhibited by EGTA and augmented by higher calcium concentrations in the medium (data not shown). Intra-cellular calcium assays demonstrated that initial increases in intra-cellular calcium occurring within 1 min of A23187 treatment were comparable between the two cell lines, while decreases in intra-cellular calcium were more rapid in HL60 cells than in CEM cells, possibly indicating differences among the two cell lines in the mechanisms of pumping out or sequestration into the intracellular organelle of calcium. These data indicate that A23187 induces a rapid influx of calcium into the cytoplasm and a slow decrease in intra-cellular calcium in CEM cells, which triggers mitochondria to undergo the morphological changes associated with necrosis. In contrast, A23187 induces a rapid influx of calcium into the cytoplasm, which rapidly decreases in HL60 cells, which are resistant to the induction of necrosis by A23187. The morphological changes, mitochondrial depolarization, and subsequent necrosis occurring in CEM cells treated with A23187 were suppressed by pre-incubation with clonazepam or CGP37157. The role of the mitochondrial permeability transition has been emphasized in the process of cell death resulting from calcium ionophore stimulation (Berridge et al., 1998; Hirsch et al., 1997; Kroemer and Reed, 2000; Lemasters et al., 1998). The mitochondrial permeability transition represents an abrupt increase in the permeability of the mitochondrial membrane, resulting from the opening of permeability transition pores in response to stimuli. Cyclosporin A specifically blocks the onset of the mitochondrial permeability transition (Lemasters et al., 1998; Nieminen et al., 1996), recognized as an important step in both necrosis and apoptosis. The mitochondrial permeability transition occurs in several forms of necrotic cell death, acting as a causative factor under some circumstances (Kroemer and Reed, 2000; Lemasters et al., 1998; Velde et al., 2000). In cultured rat hepatocytes, 10 μM Br-A23187 increased intra-mitochondrial calcium, inducing necrotic cell killing within 1 h (Qian et al., 1999). The induction of both the mitochondrial permeability transition and cell killing was prevented by 1 μM cyclosporin A, but cyclosporin A had no effect on the increase in intra-mitochondrial calcium. In Jurkat cells, cytoplasmic calcium overload induced by vanilloid receptor type1 trigger “paraptotic cell death”, which does not fulfill the criteria for either apoptosis or necrosis (Jambrina et al., 2003). The mitochondrial permeability transition and collapse of the mitochondrial membrane potential occur in this type of cell death, which is inhibited by cyclosporin A treatment.

In our study, cytoplasmic calcium overload induced by A23187 induced necrotic cell death in CEM cells, an effect which was prevented by clonazepam and CGP37157 but unaffected by cyclosporin A. The induction of necrotic death by A23187 in CEM cells is independent of the mitochondrial permeability transition, as indicated by the lack of effect of cyclosporin A. Intra-mitochondrial calcium assays using rhod-2 indicated that both clonazepam and CGP37157 caused sequestration of calcium in mitochondria, inducing increases in intra-mitochondrial calcium. Increased intra-mitochondrial calcium levels seem to protect CEM cells from the induction of necrosis by rapid increases of intra-cellular calcium. The suppression of necrotic death by an agent affecting the mitochondrial calcium level also suggests the involvement of mitochondria in this form of necrotic death. Bcl-2 shows anti-apoptotic effects in various cells and the Bcl-2 expression level in various cells determines the mode of cell death (Adachi et al., 1997; Melihac et al., 1999; Zhu et al., 1999). Caspase-independent necrosis-like cell death is also inhibited by Bcl-2 (Kitanaka and Kuchino, 1999; Jambrina et al., 2003). In neural cells, mitochondria of Bcl-2-overexpressing cells have enhanced capacity of Ca^{2+} uptake, which have greater resistance to Ca^{2+} induced injury (Murphy et al., 1996). Although the level of Bcl-2 expression assessed by Western blotting was comparable between our HL60 and CEM cells (data not shown), Bcl-2 in the outer mitochondrial membrane may play some role in this process. Bcl-2-overexpressing CEM cells showed increased necrosis in comparison with control CEM cells in response to A23187 stimulation, while the increase in intra-cellular and intra-mitochondrial calcium was similar in both cell lines.

We have previously reported that mitochondrial function is disturbed in the early phases of apoptosis (Adachi et al., 1997, 1998). Here, we demonstrated that mitochondrial dysfunction is observed early in the induction of necrosis. The precise mechanism of the complete suppression of cell death is not known, because clonazepam and CGP37157

increased intra-mitochondrial calcium levels of both CEM and HL60 cells but this intra-mitochondrial calcium increase did not inhibit cell death in HL60 cells. One possibility is that clonazepam and CGP37157 inhibited necrosis in CEM cells from different mechanism from inhibition of the mitochondrial Na^+/Ca^{2+} exchanger. Clonazepam and CGP37157 may also inhibit plasmalemmal Na^+/Ca^{2+} exchanger, which also have some effect on necrosis (Czyz and Kiedrowski, 2003; Omelchenko et al., 2003). In order to clarify the effect of Na^+/Ca^{2+} exchanger inhibitors on plasmalemmal Na^+/Ca^{2+} exchanger isoforms, we compared the early necrotic changes of CEM cells by A23187 in the Hanks solution and the Hanks solution in which NaCl was replaced with choline chloride. Those early necrotic changes in response to A23187 were similarly observed in the Na^+-abscent medium (data not shown). We then examined the expression levels of Na^+/Ca^{2+} exchanger isoforms in CEM and HL60 cells by Western blotting. In CEM and HL60 cells, expression of NCX isoforms 1, 2, 3 was not detected, which are expressed in the mouse brain or ventricular muscle tissues. Therefore the inhibitory effect of clonazepam does not appear to occur via plasmalemmal Na^+/Ca^{2+} exchanger. There has been identified that two distinct benzodiazepine binding sites, a central site restricted to brain and a ubiquitously expressed binding site, the so-called peripheral benzodiazepine receptor (Braestrup and Squires, 1977). Clonazepam are widely used as tranquilizers or anticonvulsants and these effects are primarily mediated via the central benzodiazepine receptors located in the central nervous system (Tallman et al., 1980). There are some reports that peripheral benzodiazepine receptor are related to apoptosis (Castedo et al., 2002; Gidon-Jengirard et al., 1999). Although clonazepam has a low binding affinity of peripheral benzodiazepine receptor, it may have some effect of inhibition of cell death through peripheral benzodiazepine receptor because clonazepam and other peripheral benzodiazepine receptor agonists equally inhibited rat microglia neuronal degeneration induced by lipopolysaccharide (Wilms et al., 2003).

Phospholipases are also shown to be implicated in necrotic cell death (Pilitsis et al., 2002). We then examined if phospholipase activation was observed in CEM cells treated with A23187. Phospholipase activation was not observed in CEM cells treated with A23187. A23187 induced necrotic change seems to be independent of phospholipase activation.

The early necrotic change induced by A23187 in CEM cells is independent of mitochondrial permeability transition, and may involve an alternate pathway that is affected by intra-mitochondrial calcium and that eventually disrupts mitochondrial function.

Acknowledgements

We thank Dr. Roberta A. Gottlieb (The Scripps Research Institute) for critical discussions.

References

Adachi, S., Cross, A.W., Babior, B.M., Gottlieb, R.A., 1997. Bcl-2 and the outer mitochondrial membrane in the inactivation of cytochrome c during Fas-mediated apoptosis. J. Biol. Chem. 272, 21878–21882.

Adachi, S., Gottlieb, R.A., Babior, B.M., 1998. Lack of release of cytochrome c from mitochondria into cytosol early in the course of Fas-mediated apoptosis of Jurkat cells. J. Biol. Chem. 273, 19892–19894.

Akiba, S., Ii, H., Yoneda, Y., Sato, T., 2004. Translocation of phospholipase A2 to membranes by oxidized LDL and hydroxyoctadecadienoic acid to contribute to cholesteryl ester formation. Biochim. Biophys. Acta 1686, 77–84.

Berridge, M.J., Bootman, M.D., Lipp, P., 1998. Calcium—a life and death signal. Nature 395, 645–648.

Blagosklonny, M.V., 2000. Cell death beyond apoptosis. Leukemia 14, 1502–1508.

Braestrup, C., Squires, R.F., 1977. Specific benzodiazepine receptors in rat brain characterized by high-affinity (3H)diazepam binding. Proc. Natl. Acad. Sci. U. S. A. 74, 3805–3809.

Castedo, M., Perfettini, J.L., Kroemer, G., 2002. Mitochondrial apoptosis and the peripheral benzodiazepine receptor: a novel target for viral and pharmacological manupulation. J. Exp. Med. 196, 1121–1125.

Chi, S., Kitanaka, C., Noguchi, K., Mochizuki, T., Nagashima, Y., Shirouzu, M., Fujita, H., Yoshida, M., Chen, W., Asai, A., Himeno, M., Yokoyama, S., Kuchino, Y., 1999. Oncogenic Ras triggers cell suicide through the activation of a caspase-independent cell death program in human cancer cells. Oncogene 18, 2281–2290.

Czyz, A., Kiedrowski, L., 2003. Inhibition of plasmalemmal Na^+/Ca^{2+} exchange by mitochondrial Na^+/Ca^{2+} exchange inhibitor Drosophila Na^+/Ca^{2+} exchangers by 7-chloro-5-(2-chlorophenyl)-1,5-dihydro-4,1-benzothiazepine-2(3H)-one in cerebellar granule cells. Biochem. Pharmacol. 66, 2409–2411.

Fanelli, C., Coppola, S., Barone, R., Colussi, C., Gualandi, G., Volpe, P., Ghibelli, L., 1999. Magnetic fields increase cell survival by inhibiting apoptosis via modulation of Ca^{2+} influx. FASEB J. 13, 95–102.

Fiers, W., Bayaert, R., Declercq, W., Vandenabeele, P., 1999. More than one way to die: apoptosis, necrosis and reactive oxygen damage. Oncogene 18, 7719–7730.

Gidon-Jengirard, C., Solito, E., Hoffmann, A., Russo-Marie, F., Freyssinet, J.M., Martinez, C., 1999. Annexin V counteracts apoptosis while inducing Ca^{2+} influx in human lymphocytic T cells. Biochem. Biophys. Res. Commun. 265, 709–715.

Griffiths, E.J., Wei, S.K., Haigney, M.C.P., Ocampo, C.J., Stern, M.D., Silverman, H.S., 1997. Inhibition of mitochondrial calcium efflux by clonazepam in intact single rat cardiomyocytes and effects on NADH production. Cell Calcium 21, 321–329.

Hirsch, T., Marchetti, P., Susin, S.A., Dallaporta, B., Zamzami, N., Marzo, I., Geuskens, M., Kroemer, G., 1997. The apoptosis-necrosis paradox. Apoptogenic proteases activated after mitochondrial permeability transition determine the mode of cell death. Oncogene 15, 1573–1581.

Ichas, F., Mazat, J.P., 1998. From calcium signaling to cell death: two conformations for the mitochondrial permeability transition pore. Switching from low- to high-conductance state. Biochim. Biophys. Acta 1366, 33–50.

Iwamoto, T., Pan, Y., Wakabayashi, S., Imagawa, T., Yamanaka, H.I., Shigekawa, M., 1996. Phosphorylation-dependent regulation of cardiac Na^+/Ca^{2+} exchanger via protein kinase C. J. Biol. Chem. 271, 13609–13615.

Jambrina, E., Alonso, R., Alcalde, M., Rodriguez, M.C., Serrano, A., Martinez, A.C., Garcia-Sancho, J., Izquierdo, M., 2003. Calcium influx through receptor-oriented channel induces mitochondria-triggered paraptotic cell death. J. Biol. Chem. 278, 14145–14314.

Kitanaka, C., Kuchino, Y., 1999. Caspase-independent programmed cell death with necrotic morphology. Cell Death Differ. 6, 508–515.

Kroemer, G., Reed, J.C., 2000. Mitochondrial control of cell death. Nat. Med. 6, 513–519.

Leist, M., Jaattela, M., 2001. Four deaths and a funeral: from caspases to alternative mechanisms. Nat. Rev., Mol. Cell Biol. 2, 1–10.

Lemasters, J.J., Nieminen, A.L., Qian, T., Trost, L.C., Elmore, S.P., Nishimura, Y., Crowe, R.A., Bradham, C.A., Brenner, D.A., Herman, B., 1998. The mitochondrial permeability transition in cell death: a common mechanism in necrosis, apoptosis and autophagy. Biochim. Biophys. Acta 1366, 177–196.

Matsubara, K., Kubota, M., Kuwakado, K., Hirota, H., Wakazono, Y., Okuda, A., Bessho, R., Lin, Y.W., Adachi, S., Akiyama, Y., 1994. Variable susceptibility to apoptosis induced by calcium ionophore in hybridomas between HL60 promyelocytic and CEM T-lymphoblastic leukemia cell lines: relationship to constitutive Mg^{2+}-dependent endonuclease. Exp. Cell Res. 213, 412–417.

Melihac, O., Escargueil-Blanc, I., Thiers, J.C., Salvayre, R., Negre-Salvayre, A., 1999. Bcl-2 alters the balance between apoptosis and necrosis, but does not prevent cell death induced by oxidized low density lipoproteins. FASEB J. 13, 485–494.

Muriel, M.P., Lambeng, N., Darios, F., Michel, P.P., Hirsch, E.C., Agid, Y., Ruberg, M., 2000. Mitochondrial free calcium levels (Rhod-2 fluorescence) and ultrastructural alterations in neuronally differentiated PC12 cells during ceramide-dependent cell death. J. Comp. Neurol. 426, 297–315.

Murphy, A.N., Bredesen, D.E., Cortopassi, G., Wang, E., Fiskum, G., 1996. Bcl-2 potentiates the maximal calcium uptake capacity of neural cell mitochondria. Proc. Natl. Acad. Sci. U. S. A. 93, 9893–9898.

Nieminen, A.L., Petrie, T.G., Lemasters, J.J., Selman, W.R., 1996. Cyclosporin A delays mitochondrial depolarization induced by *N*-methyl-D-aspartate in cortical neurons: evidence of the mitochondrial permeability transition. Neuroscience 75, 993–997.

Omelchenko, A., Bouchard, R., Le, H.D., Choptiany, P., Visen, N., Hnatowich, M., Hryshko, L.V., 2003. Inhibition of canine and Drosophila Na^+/Ca^{2+} exchangers by 7-chloro-3,5-dihydro-5-phenyl-1H-4,1-benzothiazepine-2-one. J. Pharmacol. Exp. Ther. 306, 1050–1057.

Pilitsis, J.G., Diaz, F.G., O'Regan M, H., Phillis, J.W., 2002. Inhibition of mitochondrial Na^+/Ca^{2+} exchange by 7-chloro-5-dihydro-5-(2-chlorophenyl)-1,5-dihydro-4,1-benzothiazepine-2(3H)-one attenuates free fatty acid efflux in rat cerebral cortex during ischemia-repurfusion injury. Neurosci. Lett. 321, 1–4.

Qian, T., Herman, B., Lemasters, J.J., 1999. The mitochondrial permeability transition mediates both necrotic and apoptotic death of hepatocytes exposed to Br-A23187. Toxicol. Appl. Pharmacol. 154, 117–125.

Scanlon, J.M., Brocard, J.B., Stout, A.K., Reynolds, I.J., 2000. Pharmacological investigation of mitochondrial Ca^{2+} transport in central neurons: studies with CGP-37157, an inhibitor of the mitochondrial Na^+–Ca^{2+} exchanger. Cell Calcium 28, 317–327.

Tallman, J.F., Paul, S.M., Skolnick, P., Gallager, D.W., 1980. Receptors for the age of anxiety: pharmacology of the benzodiazepines. Science 207, 274–281.

Toyokuni, S., Okada, S., Hamazaki, S., Fujioka, M., Li, J.L., Midorikawa, O., 1989. Cirrhosis of the liver induced by cupric nitrilotriacetate in Wister rats. An experimental model of copper toxicosis. Am. J. Pathol. 134, 1263–1274.

Velde, C.V., Cizeau, J., Dubic, D., Alimonti, J., Brown, T., Israels, S., Hakem, R., Greenberg, A.H., 2000. BNIP3 and genetic control of necrosis-like cell death through the mitochondrial permeability transition pore. Mol. Cell. Biol. 20, 5454–5468.

Wilms, H., Claasen, J., Rohl, C., Sievers, J., Deuschl, G., Lucius, R., 2003. Involvement of benzodiazepine receptors in neuroinflammatory and neurodegenerative diseases: evidence from activated microglial cells in vitro. Neurobiol. Dis. 14, 417–424.

Yamashita, K., Takahashi, A., Kobayashi, S., Hirata, H., Mesner Jr., P.W., Kaufmann, S.H., Yonehira, S., Yamamoto, K., Uchiyama, T., Sasada, M., 1999. Caspases mediate tumor necrosis factor-α-induced neutrophil apoptosis and downregulation of reactive oxygen production. Blood 93, 674–685.

Zhu, W.H., Loh, T.T., 1995. Roles of calcium in the regulation of apoptosis in HL60 promyelocytic leukemia cells. Life Sci. 57, 2091–2099.

Zhu, L., Ling, S., Yu, X.D., Venkatesh, L.K., Subramanian, T., Chinnadurai, G., Kuo, T.H., 1999. Modulation of mitochondrial Ca^{2+} homeostasis by Bcl-2. J. Biol. Chem. 274, 33267–33273.